A METHODOLOGICAL APPROACH FOR THE EFFECTIVE INFILTRATION ASSESSMENT IN A COASTAL GROUNDWATER

Maria Chiara PORRU[(*)], Stefania DA PELO[(*)], Stephen WESTENBROEK[(**)], Andrea VACCA[(*)]
Alfredo LOI[(*)], Maria Teresa MELIS[(*)], Arianna PIRELLAS[(*)], Cristina BUTTAU[(*)],
Claudio ARRAS[(*)], Salvatore VACCA[(*)], Maria Luisa MASON[(***)], Mario LORRAI[(****)]
Maurizio TESTA[(*****)] & Paolo BOTTI[(****)]

[(*)]University Campus of Cagliari - Department of Chemical and Geological Sciences, Building A - 09042 Monserrato (Cagliari, Italy)
[(**)]U.S. Geological Survey - Wisconsin Water Science Center, Middleton - WI 53562 (United States)
[(***)]Freelance
[(****)]Regione Autonoma della Sardegna, Servizio tutela e gestione delle risorse idriche, vigilanza sui servizi idrici e gestione delle siccità
- Via Mameli, 88 - 09123 Cagliari (Italy)
[(*****)]Regional Environmental Protection Agency of Sardinia (ARPA Sardegna) - Via Contivecchi, 7 - 09122 Cagliari (Italy)
Corresponding author: sdapelo@unica.it

EXTENDED ABSTRACT

Gli acquiferi costieri rappresentano sistemi estremamente sensibili a fenomeni di intrusione salina a causa dell'eccessivo sfruttamento delle risorse idriche e degli effetti dei cambiamenti climatici. Per implementare un sistema di gestione integrato e sostenibile volto sia a rallentare il processo di intrusione di acqua salata che a soddisfare i fabbisogni antropici ed ecosistemici, è importante sviluppare un sistema di analisi flessibile, adatto a diversi scenari, che tenga conto dei cambiamenti dell'uso del suolo e dell'assetto idrogeologico, anche in relazione al cambiamento climatico. Risulta pertanto fondamentale conoscere e quantificare in maniera accurata la distribuzione della ricarica.

In questo studio, è stato applicato l'innovativo codice Soil Water Balance (SWB) per calcolare le variazioni spaziali e temporali della ricarica delle acque sotterranee nell'area pilota di Muravera. La piana costiera di Muravera, nella Sardegna sud-orientale, è stata studiata fin dal 1960, in quanto soggetta all'intrusione di acqua di mare che ha causato sia la salinizzazione dell'acquifero alluvionale che del suolo, con la perdita dei terreni tradizionalmente utilizzati per l'agricoltura. Dall'inizio degli anni cinquanta, l'equilibrio idrodinamico naturale tra acque sotterranee, acque superficiali e acque marine è stato profondamente modificato da varie opere di ingegneria fluviale e dallo sviluppo di attività agricole, turistiche e di acquacoltura lungo la costa. Il codice SWB applicato in questo lavoro calcola la ricarica (R) utilizzando livelli di dati generati in ambiente GIS in combinazione con dati climatici tabulari. Si basa su un approccio di equilibrio suolo-acqua Thornthwaite - Mather modificato, con le componenti del bilancio idrico del suolo calcolate su base giornaliera. Per la stima dei dati necessari per l'implementazione del codice è stato applicato un approccio sperimentale combinato con metodologie idrogeologiche, di telerilevamento satellitare e pedologiche acquisendo dati misurati in situ, in laboratorio e da remoto. Nello specifico, lo studio è stato suddiviso in tre fasi, partendo dai rilevi geologici e pedologici effettuati in precedenti studi: (1) sono state svolte diverse prove infiltrometriche sul campo per la valutazione della conducibilità idraulica allo stato saturo, e sono stati raccolti campioni di terreno, (2) sono state effettuate analisi di laboratorio sui campioni prelevati al fine della determinazione di: granulometria, contenuto di acqua, peso specifico e porosità dei terreni, (3) è stata elaborata la carta della copertura del suolo da dati da satellite, validati con rilievi in campo per la verità a terra, attraverso i quali è stato possibile valutare la capacità di infiltrazione dei suoli e determinare la ricarica diretta delle acque sotterranee nell'area di Muravera. Questo ha permesso di creare i file di input in formato grid richiesti dal SWB: (1) uso del suolo, (2) gruppo idrologico del suolo, (3) direzione del flusso e (4) capacità di campo.

Lo studio, ha consentito di fornire ulteriori dati sulle caratteristiche idrologiche dei suoli locali. È risultato evidente che le pratiche agricole, il pascolo e il grado di saturazione dei suoli influenzano il tasso di infiltrazione. Infatti, a parità di condizioni di tessitura, i terreni arati hanno mostrato una conducibilità satura più elevata, mentre i terreni sottoposti a calpestio da parte dei pascoli hanno mostrato un tasso di infiltrazione inferiore. Dal bilancio idrogeologico calcolato, le zone di maggiore infiltrazione sono state riscontrate in corrispondenza dei depositi quaternari. Gli input grid file richiesti dal SWB hanno permesso di conoscere la spazializzazione di diversi dati e quindi di aumentare il livello di conoscenza dell'area di studio. Uno dei maggiori vantaggi di SWB è la sua semplicità e velocità di utilizzo. Sebbene il SWB non consideri il flusso nella zona insatura, nella piana di Muravera la profondità del livello delle acque sotterranee non supera i 2-3 metri, pertanto si può ipotizzare che l'intervallo di tempo che intercorre tra il momento in cui SWB genera la ricarica e il momento in cui tale ricarica raggiunge effettivamente la falda freatica sia trascurabile. L'applicazione del SWB alla piana di Muravera è un importante test della capacità del modello SWB di stimare la ricarica in un'area mediterranea con diversi usi del suolo, e in generale con elevata capacità di infiltrazione. Questo metodo è risultato adatto per l'applicazione in aree e casi simili e ha fornito risultati molto utili per gestire al meglio le risorse idriche della piana. E' stato infatti possibile valutare le zone di maggiore infiltrazione e quindi individuare le zone in cui avviene la massima ricarica delle acque sotterranee. Il codice si è dimostrato promettente per l'efficace valutazione dell' infiltrazioni e può essere facilmente aggiornato con i dati ad alta risoluzione acquisiti sul campo e da immagini satellitari, e anche utilizzato per valutare scenari futuri.

M.C. PORRU, S. DA PELO, S. WESTENBROEK, A. VACCA, A. LOI, M.T. MELIS, A. PIRELLAS, C. BUTTAU, C. ARRAS, S. VACCA, M.L. MASON, M. LORRAI, M. TESTA & P. BOTTI

ABSTRACT

Accurate estimates of spatial and temporal distribution of groundwater recharge are of utmost importance to protect groundwater systems. In coastal areas, the fragility of the systems makes such estimates critical for the correct management and protection of water resources from saltwater intrusion.

The Muravera coastal plain, in the south-eastern Sardinia, has been studied since 1960, due to important saltwater intrusion phenomena. Since the early fifties, the natural hydrodynamic equilibrium between groundwater, surface-water and seawater has been deeply modified by the construction of four dams across the Flumendosa river and the development of agriculture, tourism and aquaculture activities along the coast. To implement an integrated and sustainable management system addressed to slow down the process of saltwater intrusion and, on the other, satisfy human requirements, it is important to develop a flexible scenario analysis system that considers changes of land-use and inputs to the hydrogeological system, also in relation to climate change.

In this study, the innovative Soil Water Balance code (SWB) has been applied to the Muravera plain groundwater body to calculate spatial and temporal variations of groundwater recharge. The code calculates the recharge (R) by using geographic system (GIS) data layers in combination with tabular climatological data. It is based on a modified Thornthwaite - Mather soil water balance approach, with components of the soil water balance calculated at a daily time-step.

A combined experimental approach of hydrogeological, satellite remote sensing and pedological methodologies has been applied to derive data layers describing local features of: (1) land-use classification, (2) hydrologic soil group, (3) flow direction, and (4) soil-water capacity.

The code has proved to be promising for the effective infiltration assessment and it can be easily updated with high resolution data acquired in the field and from satellite images.

KEYWORDS: saltwater intrusion, Soil Water Balance, groundwater

INTRODUCTION

Over-exploitation of groundwater resources and the effects of climate change are increasing pressures on coastal areas all over the world, making them very vulnerable to saline intrusion (BARLOW & REICHARD, 2010; COLOMBANI *et alii*, 2016; CRAMER *et alii*, 2018). In the alluvial plain of Muravera, along the mouth of the Flumendosa river, the saltwater intrusion has led both to the salinization of the coastal aquifers of the plain, but also to the accumulation of salt in soils, with the loss of land traditionally used for agriculture. Especially in summer when demand increases due to drought, salt water has progressively invaded the inland. The balance between fresh and salt water has been modified mainly by human activity and by the various river

engineering works. Indeed, water supply throughout the area has always been guaranteed by an increasing number of wells in the plain subject to uncontrolled groundwater abstractions. Following the construction of four dams, a drastic decrease in river outflow into the mouths has been generated. In addition, at the beginning of the last century, embankments were built that blocked the water circulation of the Flumendosa river in three arms. Currently, following the artificial openings of the fishpond of San Giovanni, the three arms, are in direct contact with the sea. In this context, the development of an integrated and sustainable groundwater management model is extremely critical and is of primary importance not only for the protection of the environment but also for the health of inhabitants and for social, economic and territorial development. It is therefore essential to know and quantify the sources and recharging mechanisms. Many methods of estimating groundwater recharge have been developed in the literature for application to problems of water supply, water quality and agriculture (e.g., SCANLON *et alii*, 2002; NIMMO *et alii*, 2005, JIE *et alii*, 2011). Despite the growing demand for hydrological assessments in support decisions systems, estimation of groundwater recharge remains a major challenge in hydrogeological studies (CHEMINGUI *et alii*, 2015). The aim of the work was the application of the Soil Water Balance (SWB) method to support the groundwater resources management.

The SWB code has been developed to allow estimates of groundwater recharge to be made quickly and easily. The code calculates components of the water balance at a daily timestep by means of a modified version of the Thornthwaite–Mather soil-water balance approach (THORNTHWAITE & MATHER, 1957; WESTENBROEK *et alii*, 2018). Recharge estimates calculations are made on a grid of computational elements that may be easily imported into a groundwater-flow model.

This study was divided into three phases:
- in the first, a soil infiltration tests survey was carried out on the basis of results from previous studies on the characterization of the soils in the Muravera coastal plain (MASON, 1999). Samples of soils at each test site were collected.
- in the second, laboratory analyses were carried out on the samples taken in the area during the infiltration tests. Water content, dry density and particle density of the samples were determined, and porosity of soils were calculated. The samples taken were also analysed for grain size distribution. The acquired data were used for the creation of the grid maps to be implemented in the SWB software.
- in the last phase, through the SWB software, the data were processed to assess the infiltration capacity of the soils and calculate the direct groundwater recharge in the Muravera area. The average annual recharge has been

assessed through a hydrological balance considering the properties of the soil and their uses. With the data collected through infiltration tests and laboratory tests, it has been possible to evaluate the areas of major infiltration and then identify the areas in which the maximum direct groundwater recharge occurs.

SITE CHARACTERIZATION

Geological setting

The Muravera coastal plain (South-eastern Sardinia) consists of Pleistocene and Holocene alluvium up to a few hundred meters thick and overlaying the metamorphic and granitic Paleozoic bedrock outcroppings at its edges (Fig. 1).

The most ancient formation, the "Arenarie di San Vito" Fm., is composed of a thick, weakly metamorphosed sequence of sandstone and shales. The foothills encompassing the plain are

The Quaternary deposits of the Upper Pleistocene and the Holocene fill the alluvial plain by superimposing themselves on the basement in the foothills, while in the central-eastern part there is a deposit of coastal plain facies. Below the Holocene alluvial deposits and in heteropic contact with the fans, a thick clayey succession, dark grey in colour, was found, with intercalated sandy and pebbly levels.

Hydrogeological setting

The river and some of its main tributaries were dammed upstream, so that the natural recharge of the coastal aquifers has now decreased significantly, and the mouth channels, which once drained groundwater, now contain saltwater coming directly from the sea. Furthermore, phreatic and deep aquifers are being increasingly exploited through wells that are being excavated and drilled to meet the ever-growing water demand for agriculture
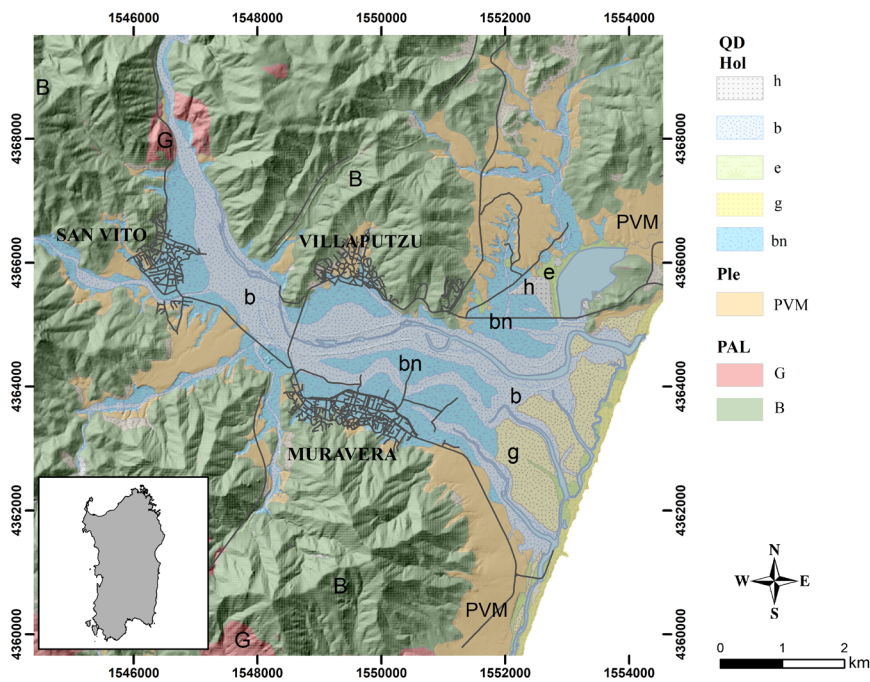

Fig. 1 -   Geological map of the Muravera plain. www.SardegnaGeoportale.it. Legend: QD) Quaternary Deposits; Hol) Holocene deposits; h) Anthropic deposits; b) Alluvial deposits (gravel and sand); e) Lake deposits (silt and clay); g) Beach deposits (sand); bn) Terraced alluvial deposits (gravel and sand); Ple) Pleistocene; PVM) Pleistocenic alluvial deposits (gravel and sand); PAL) Paleozoic; G) Unsorted granitoids; B) Metamorphic basement

composed entirely of clastic sediments (alluvial fan) that further down-slope mingle with the ancient alluvium bordering the water courses. The river valley floor and the entire plain are made up of recent and actual alluvium (ARDAU & BARBIERI, 2000).

In the eastern portion of the plain, the Paleozoic basement is found at depths of several hundred meters from the ground level, below the cover deposits; in the upstream area and in correspondence with the secondary hydrographic network, it is found a few tens of meters below the ground level.

and domestic uses, mainly in summer.

A complex multilayer aquifer, partly phreatic and locally confined, characterizes the hydrogeological structure. It consists largely of loose coarse alluvial deposits, which allow a usually high water circulation due to primary porosity. Locally, the presence of a clayey body hydraulically separates the deposit, giving rise to a shallow groundwater aquifer and a locally confined deeper aquifer. The Palaeozoic basement is the lower limit of alluvial deposits in the upstream area and along the edges of the alluvial

M.C. PORRU, S. DA PELO, S. WESTENBROEK, A. VACCA, A. LOI, M.T. MELIS, A. PIRELLAS, C. BUTTAU, C. ARRAS, S. VACCA,
M.L. MASON, M. LORRAI, M. TESTA & P. BOTTI

plain. The Palaeozoic basement is quite impermeable even if locally, in the main areas of alteration and fracture, a certain water circulation may take place. The alluvial fans in the foothills host an aquifer characterized by a certain degree of consolidation and cementation that allow a moderate water circulation for primary porosity. Moving towards the central portions of the plain, the conoids deepen.

Soil groups occurrence (sensu IUSS WORKING GROUP WRB, 2015)

Distribution of soil types varied with landform and parent material (CALZOLARI et alii, 2021). The great lithological and morphological variability that characterizes the area is reflected in a good taxonomic variability. In highland, where steeper slopes occur, mainly very weakly (Leptosols and Regosols) and weakly (Cambisols) developed soils are present, mainly linked to the metamorphic basement (MET, Fig. 2). Deeper soils (Regosols and Cambisols) occur where morphological character allows depositional processes prevailing on erosional. In lowland flat areas, alluvial and floods sediments transported by the Flumendosa river and its main tributaries predominate. Pedological characteristics reflect different dynamics controlling the alluvial and flood sediments deposition and the age of parent material. The soils formed on recent floods have a clayey texture (ALO and SLO, Fig. 2), often sandy (ASO and ATS, Fig. 2), little skeleton and are rich in organic matter. The soils closest to the coastline and to the lagoon areas have been recognized as Sodic Salic Cambisols, mainly due to the high electrical conductivity values. At the edges of the alluvial plains and along the main tributaries there are sediments characterized by torrential depositions, not very elaborate, terraced, in often sandy matrix, mixed with gravelly colluvial deposits, sometimes pebbly, in clayey matrix (DAP, AGO and ATG, Fig. 2). In these areas, Regosols, Cambisols and Fluvisols prevail on Holocene deposits (AGO and ATG), while more developed soils (mainly Luvisols) largely prevail on Pleistocene deposits (DAP). All these soils are generally deep, sandy loam throughout (Regosols, Cambisols and Fluvisols) or sandy loam on the surface and more clayey in depth (Luvisols).

MATERIALS AND METHODS
Sampling and analysis of soil

In situ infiltration tests by the double ring infiltrometer (EIJKELKAMP COMPANY, 2012) were carried out for the determination of field-saturated hydraulic conductivity at 11 measure stations, according to the occurrence of different parent materials and soil types, as indicated in Fig. 2.

For the assessment of the reproducibility of the double ring infiltrometer measurements, three simultaneous tests were carried out at two sites in an area of about 30x30 m. The analysis of the replicated measurements showed a variability of the data ranging between 20 and 40%.

During the test the water level has been measured with increasing times following a geometric progression (e.g.: 15seconds/30seconds/60seconds/120seconds/240seconds/..).

At the end of the test, two samples were collected with a cutting die of a known volume for soil index properties characterizations, one, saturated, within the area of the ring test (Internal samples) and one, with natural humidity, outside the measurement system (External samples). A third sub-sample was also collected at each test point for particle size characterization. At selected sites, a soil profile was opened and samples were collected from the different soil horizons in order to measure the grain size distribution.

The hydraulic conductivity was estimated according to the Kostiakov power law for the evaluation of the cumulative infiltration at any time t (KOSTIAKOV, 1932):

$$I_C = at^b$$

where a and b are two experimentally determined constants and t is the time. The infiltration rate was calculated as the incremental ratio between cumulate infiltration and the time, thus the first derivative of the KOSTIAKOV power law:

$$dI_C/dt = bat^{(b-1)}$$

As time increases, the infiltration rate approaches zero instead of a constant (non-zero) value (NIGRELLI, 2000).

The laboratory tests were carried out at the Applied Geology and Pedology laboratories of the Department of Chemical and Geological Sciences of Cagliari University.

The determination of dry density, water content, particle density and porosity, was carried out for each sample. The particle density was determined by the pycnometer. Porosity has been calculated from the dry density and particle density values, according to the formula:

$$n = 1 - (\rho_d/\rho_s)$$

n = porosity
ρ_d = dry density (g/cm³)
ρ_s = particle density (g/cm³)

Soil Water Balance

Soil Water Balance (SWB 1.2) is a computer code, developed by the USGS, based on a modified Thornthwaite-Mather soil-water balance approach. The principles of the method are described in WESTENBROEK et alii (2010). The code calculates recharge (R) by use of geographic system (GIS) data layers in combination with tabular climatological data. It is based on a
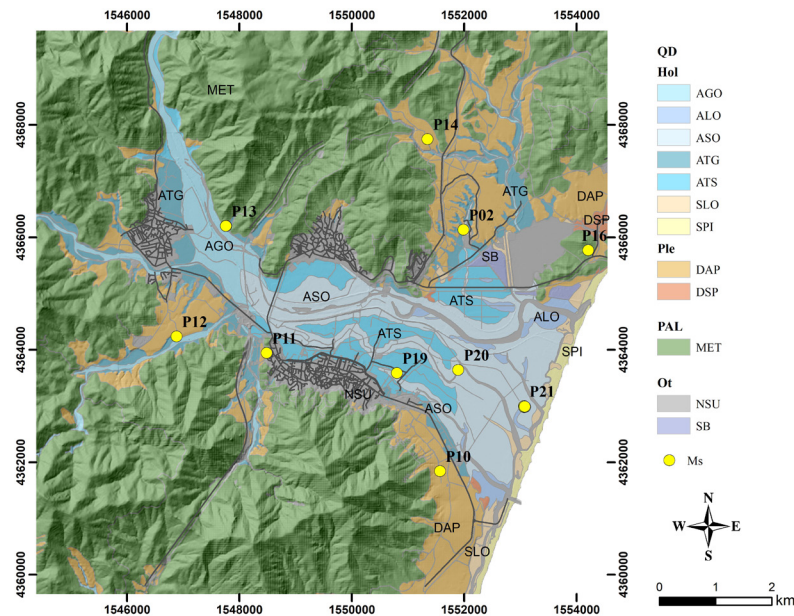
Fig. 2 - Land unit map (AGRIS et alii, 2014) and measure stations locations. Legend: QD) Quaternary Deposits; Hol) Holocene; AGO) Gravelly alluvial deposits; ALO) Clayey silty alluvial deposits; ASO) Sandy alluvial deposits; ATG) Terraced gravel deposits; ATS) Terraced sandy alluvial deposits; SLO) Clayey silty lake sediments; SPI) Wind deposited sand and sand dunes; Ple) Pleistocene; DAP) Alluvial gravel deposits; DSP) Beach deposits; PAL) Paleozoic; MET) Meta-sediments; Ot) Other; NSU) Areas of no soil; SB) Antropic deposits; Ms) Measuring stations

modified Thorntwaite-Mather soil water balance approach, with components of the soil water balance calculated at a daily time-step.

$$R = (precip + snowmelt + inflow) - Sources$$

$$(interception + outflow + ET) - \Delta\ soil\ moisture\ Sinks$$

Recharge is calculated separately for each grid cell in the model domain. Sources and sinks of water within each grid cell are determined based on input climate data and landscape characteristics; recharge is calculated as the difference between the change in soil moisture and these sources and sinks. Specific water balance components are discussed briefly below.

- Precip- Precipitation data were obtained from the ARPAS real-time monitoring network for a period of time ranging from 1st January 2006 to 31st December 2018, 12 full years.
- Snowmelt- the daily mean, maximum, and minimum air temperatures are used to determine whether precipitation takes the form of rain or snow.
- Inflow- Inflow is calculated by use of a flow direction grid derived from a digital elevation model to route outflow to adjacent downslope grid cells. The grid of flow direction has been generated from a model of digital elevation (DEM) of 10 m joining sheets 549

and 558 of the Union Framework (scale 1:50.000) extracted from the Geoportal of the Sardinia Region. Flow directions were determined using the flowdirection ArcGis command grid using a D8 flow-routing scheme.

- Interception- a user specified amount of rainfall is assumed to be trapped and used by vegetation and evaporated or transpired from plant surfaces. Interception values may be specified for each land-use type and season.
- The land cover map has been extracted from ESA Sentinel 2 imagery acquired on 02/08/2018. In this season, at the Mediterranean latitude, agriculture lands exhibit the maximum spectral contrast and a very low grade of cloud cover is found. Maximum Likelihood supervised classification methodology (MATHER *et alii*, 2001) has been applied on radiometrically corrected multispectral data with 10 m of spatial resolution. Assuming that for each land cover class in each band the statistics are normally distributed, this classification calculates the probability that a given pixel belongs to a specific class (RICHARDS, 1999). Available thematic maps and Google Earth high resolution satellite images were consulted to compare the spectral data with the ground truth (AFRASINEI *et alii*, 2015), and field/direct knowledge improved and completed the remote observations. Starting from the delimitation of the training sites for each of the 17 land cover classes, the

M.C. PORRU, S. DA PELO, S. WESTENBROEK, A. VACCA, A. LOI, M.T. MELIS, A. PIRELLAS, C. BUTTAU, C. ARRAS, S. VACCA, M.L. MASON, M. LORRAI, M. TESTA & P. BOTTI

Soil Land Unit[*1]			On site measurements				Table 6 SWB[*2]		Table 7 SWB[*2]	
Soil Units	Lithology	Texture	Station	Ksat (m/s)	Topsoil Sample	Depth of water table (m)	Soil Group	Infiltration Rate (m/s)	Texture	Water capacity (%)
AGO	Gravelly alluvial deposits	Loamy sand / Sandy	P13	2.26E-05	Loamy sand	3	A	≥2.11E-06	Sandy clay loam	22.5
ALO	Clayey silty alluvial deposits	Loam / Silty loam	P21	1.95E-06	Loam	0.1	B	1.05E-06 - 2.11E-06	Silty clay	28.3
ASO	Sandy alluvial deposits	Loamy sand / Sandy loam	P20	5.89E-06	Loamy sand	1	A	≥2.11E-06	Loamy sand	11.7
ATG	Terraced gravel deposits	Sandy loam / Loamy sand	P02	1.40E-05	Sandy clay loam	1	A	≥2.11E-06	Sandy loam	13.3
ATS	Terraced sandy alluvial deposits	Loam / Loamy sand	P19	1.80E-05	Loam	2	A	≥2.11E-06	Silty loam	20
DAP	Alluvial gravel deposits	Loamy sand / Silty loam	P10 P11 P12 P14	1.23E-04 1.72E-05 1.16E-04 1.53E-05	Loamy sand	7 5 15 -	A	≥2.11E-06	Sandy clay loam	22.5
DSP	Antique beach deposits	Clay loam / Sandy clay	P15	2.87E-06	Loamy sand	2	A	≥2.11E-06	Sandy clay loam	22.5
MET	Paleozoic metamorphites	Loam / Silty loam	P16	1.53E-06	Loamy sand	1	B	1.05E-06 - 2.11E-06	Sandy loam	23.3
NSU	No soil	-	-	-	-	-	D	-	-	30
SB	Anthropic deposits	-	-	-	-	-	C	-	-	29.2

*Tab. 1 - Synoptic table. [*1] AGRIS et alii (2014); [*2] WESTENBROEK et alii (2010)*

final classification has been validated and the overall accuracy has been calculated through the confusion matrix. In this square matrix, true classes are compared with the classifier's predictions. The overall accuracy is calculated by summing the number of correctly classified values and dividing by the total number of values. Moreover, a measure of the agreement between classification and truth values can be calculated through the Kappa coefficient. The resulting value of the overall accuracy, 86,56%, and a Kappa coefficient of 0,85 can be considered in fine agreements between the final classification and truth values. The resulting grid for land use was reclassified so that the land use codes were consistent with the modified Anderson Level II scheme originally used by DRIPPS (2003).

- Outflow- the value for each cell is derived from a curve that relates the rain to the surface runoff. This curve is calculated by use of the U.S. Department of Agriculture, Natural Resources Conservation Service (NRCS) curve number rain-fall-runoff relation (CRONSHEY, 1986). The outflow is given by the difference between precipitation and a term called "initial abstraction" that takes into account all those processes that go to intercept the precipitation water and therefore to reduce the outflow (such as infiltration, vegetation, etc.).

- Evapotranspiration- evapotranspiration has been calculated with the Thornthwaite–Mather method. Temperature data were obtained from the ARPAS real-time monitoring network for a period of time ranging

from 1st January 2006 to 31st December 2018, 12 full years.

- Δ soil moisture- The water capacity grid was created by assigning the values of available water capacity (expressed as a percentage) to soil types in the soil hydrological group grid.

- Four gridded datasets are required in the model: (1) hydrologic soil group, (2) land-use/land-cover, (3) available soil-water capacity, and (4) surface-water flow direction (Fig. 3).

RESULTS AND DISCUSSION

Particle density were similar for all samples. The values varied from a minimum of 2.57 g/cm³ in sample P16 External at a maximum of 2.71 g/cm³ in sample P13 Internal. The values of Internal and External samples at each test site were consistent, with variations of less than 2%. Porosity ranged between 0.43 to 0.55. Precision of the determinations was estimated at 10-15% by replicating samples.

Clay fractions were quite low for almost all the samples and are between 5 and 24%. Silt is the predominant fraction (between 28% and 60%), generally evenly balanced between fine and coarse silt. The sand fractions are above 30% in all samples. The soil texture doesn't change significantly at depth except for P21 where sandy fraction increases from 40% to 80% at about 80 cm below the ground level. Quite the opposite, P2 at around 100 cm depth showed an increase of clay fraction up to 50%.

Saturated hydraulic conductivity varied between 5.89E-06 m/s and 1.16E-04 m/s. The greater values were measured in soils developed on Pleistocene gravel deposits (P10 and P12 - DAP),
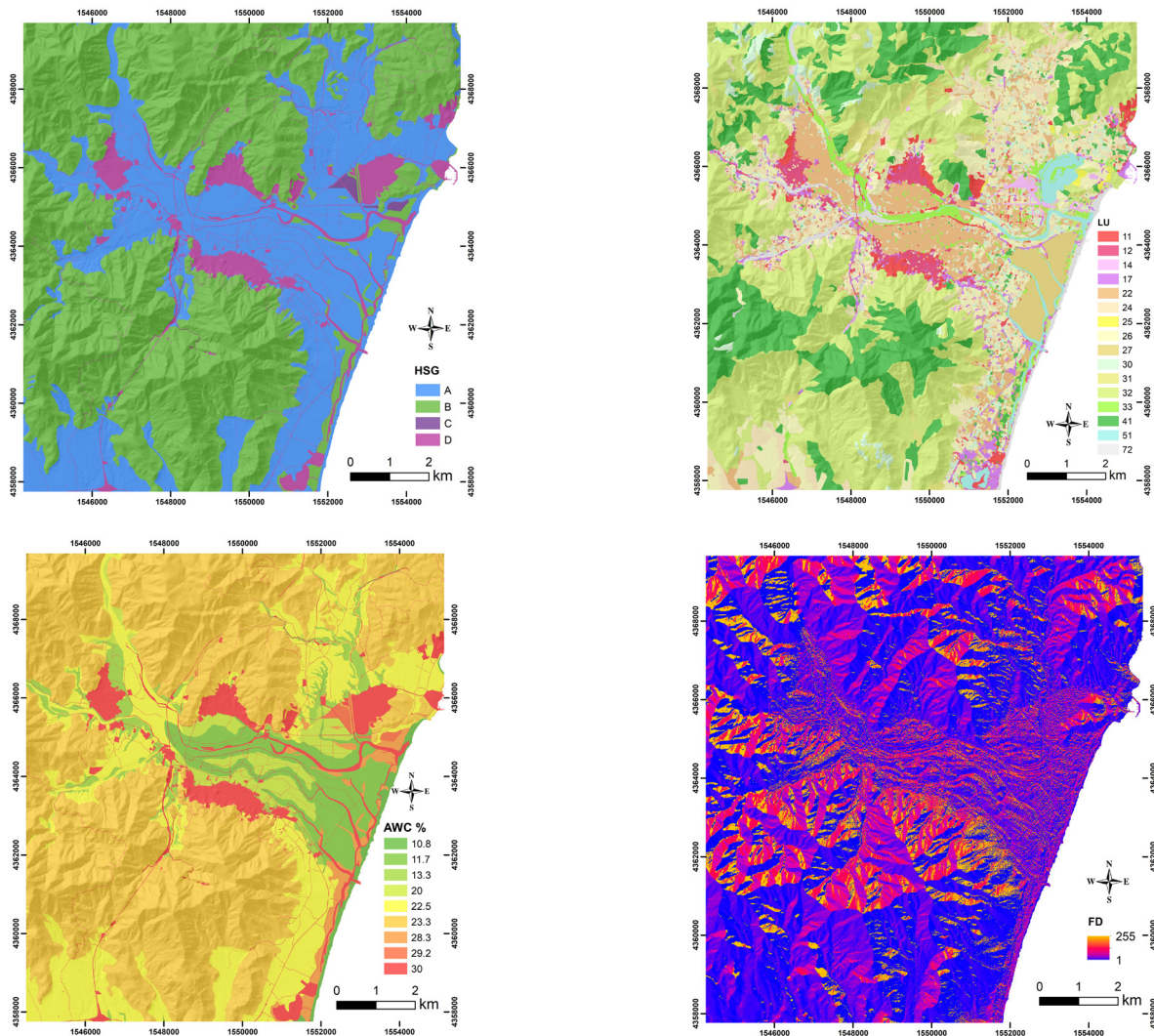
Fig. 3 - Gridded land surface data required for the application of the SWB model. Details on the data are reported in Table 1. LEGEND: top left, (HGS) Hydrologic Soil Group map; top right, (LU) Land-use map: 11) Residential, 12) Urban, 14) Artificial, non-agricultural vegetated areas, 17) Artificial surface, 22) Orchards, 24) Heterogeneous agricultural areas, 25) Shallow-rooted crops, 26) Moderately-deep crops, 27) Paddy fields and alfalfa in rotation, 30) Sparsely vegetated areas, 31) Pasture, 32) Mediterranean scrub, 33) Riparian vegetation, 41) All forest type, 51) Water bodies, 72) Sandy areas; bottom left, (AWC) Available soil water capacity; bottom right, (FD) Surface water flow direction

while the lowest was found in soils developed on metamorphic lithologies (P16) or near the Foxi (P21), where the clayey loam component is more abundant in the top soil. In some areas, high compaction was observed due to the passage of livestock (P16). The greatest permeability has been found in cultivated areas, where agricultural practices and ploughing probably prevent the compaction of soils. Infiltration rate has been evaluated as strongly dependent by the initial saturation grade of the soils.

SOIL WATER BALANCE

The results of field and laboratory tests have been implemented in the SWB model according to the classification scheme proposed by WESTENBROEK *et alii* (2010), as reported in Tab. 1. The four grids were created, including the hydrologic soil group map, the Land-use map, the available soil water capacity, and the surface water flow direction (Fig. 3).

Hydrological soil group map shows the different permeability of soils. Group A have a high infiltration capacity and, consequently, a low overland flow potential. Group A includes most of the soils of the plain.

The remaining soils sampled (falling in ALO and MET) are part of group B which has a lower infiltration rate than group

M.C. PORRU, S. DA PELO, S. WESTENBROEK, A. VACCA, A. LOI, M.T. MELIS, A. PIRELLAS, C. BUTTAU, C. ARRAS, S. VACCA, M.L. MASON, M. LORRAI, M. TESTA & P. BOTTI

A. The land-use grid map shows that most of the area has agricultural use and is occupied by crops and orchards. From the map of Available soil water capacity, it appears that the central part of the plain, corresponding to the riverbed and the abandoned branches, presents the minor Available soil water capacity (11.7-13.3%).

Natural groundwater recharge (R) was as a residual of the water balance using the following mass balance equation:

$$R = GP - Runoff - \Delta sm - Act\ ETs - Act\ ETi$$

where *GP*, *Runoff*, *Δsm*, *Act ETs* and *Act ETi* are respectively the gross precipitation, the surface flow that flows out of the model domain, the change in soil moisture, the actual evapotranspiration from the soil and the actual transpiration from the canopy that intercepts the rainfall (Tab. 2).

Figure 4 shows the recharge maps for the years 2006, 2010, 2015, 2018 as representative of the different recharge scenarios that occurred. Colour gradations indicate different levels of infiltration expressed in mm per years.

Year	input	output						
	Gross Precipitation	Recharge	Runoff	Δ soil moisture	Actual ET soil	Actual ET interception	Mass balance	Error
				Mm³				%
2006	85.75	15.17	5.27	14.41	39.81	10.43	0.66	0.77
2007	69.22	2.62	3.66	-3.72	53.16	13.60	-0.11	-0.16
2008	70.40	9.13	3.79	2.69	41.27	13.50	0.01	0.01
2009	84.28	16.64	4.61	-11.47	60.36	13.99	0.15	0.18
2010	91.19	10.45	5.08	7.63	52.28	15.91	-0.15	-0.17
2011	84.78	16.26	5.08	-0.05	50.73	12.17	0.59	0.69
2012	51.23	5.20	2.70	-9.69	42.85	10.32	-0.15	-0.30
2013	77.21	7.10	4.20	11.05	41.05	13.91	-0.11	-0.14
2014	42.68	0.38	1.97	-7.25	36.34	11.19	0.05	0.12
2015	78.98	14.04	4.56	0.23	49.32	10.81	0.02	0.03
2016	65.89	7.09	3.77	6.96	37.80	10.16	0.11	0.16
2017	37.38	5.76	2.00	-9.83	30.53	8.98	-0.06	-0.17
2018	149.71	46.73	9.88	11.11	63.43	16.15	2.41	1.61
2006-2018	76.05	12.04	4.35	0.93	46.07	12.39	0.26	0.34

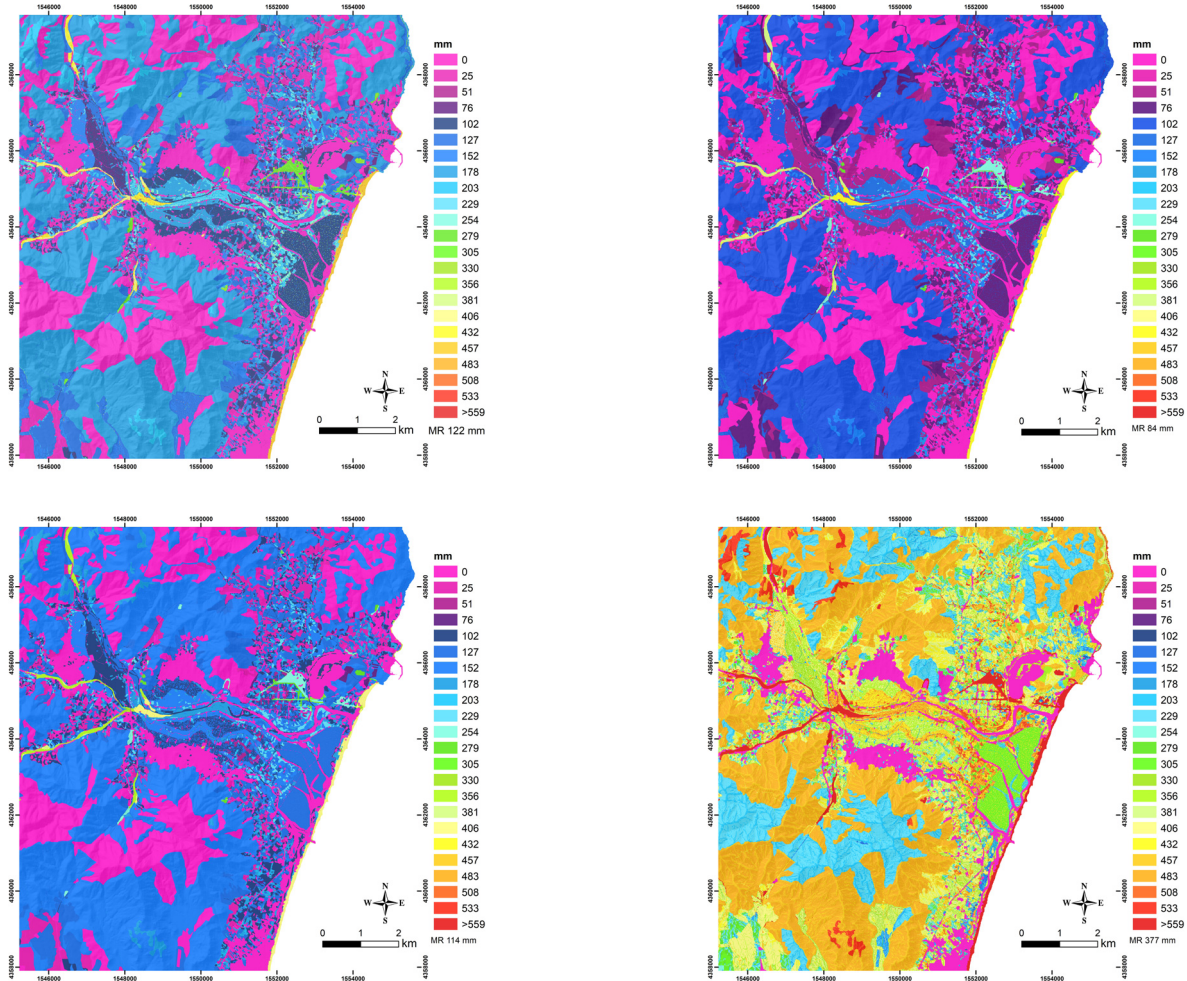*Tab. 2 - Annual mass balance for the entire domain*

Fig. 4 - Examples of some years recharge map obtained by the SWB code (data in mm). LEGEND: MR) Mean Recharge

Different average recharge rates over the years can be observed, ranging between 3 mm in 2014 and 376 mm in 2018. They represent a percent of gross precipitation ranging between the 1% and the 31% (Fig. 5). Accordingly, average, and maximum temperature in 2014 were the highest.
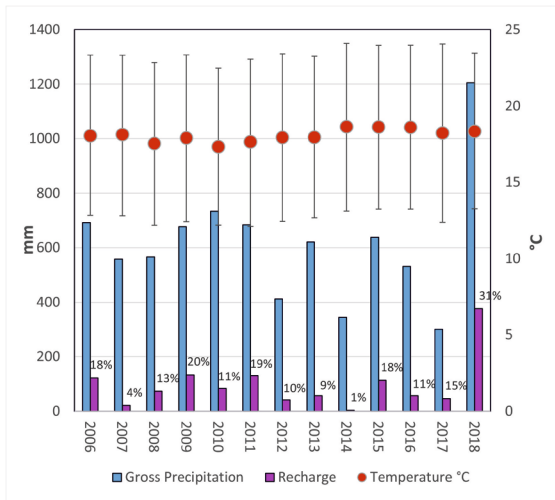

Fig. 5 -   Percentage of net recharge compared to gross precipitation and average, minimum and maximum temperature

A significant linear correlation between gross precipitation and recharge rate was recognized, indicating that generally, increasing rain precipitation recharge rate increases (Fig. 6).
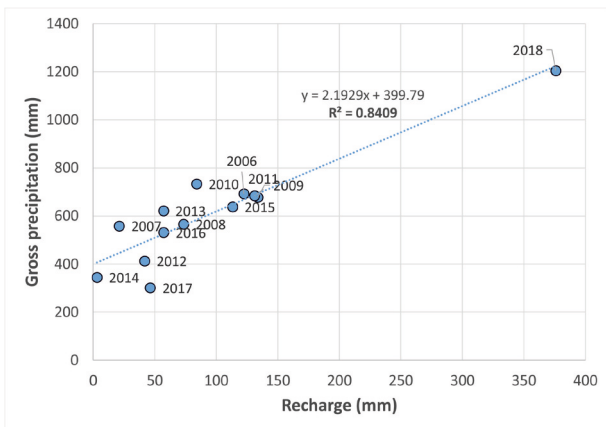
Fig. 6 -   Correlation between gross precipitation and net recharge

The resulting map of the potential direct recharge of groundwater for the period of 12 years, from 2006 to 2018, is reported in Fig. 7. The calculated hydrogeological balance shows that the maximum recharge rate occurs in the Quaternary deposits (gravel and sand), where precipitation has a higher infiltration rate. The highest mean recharge is observed at the Holocene deposits (gravel and sand).
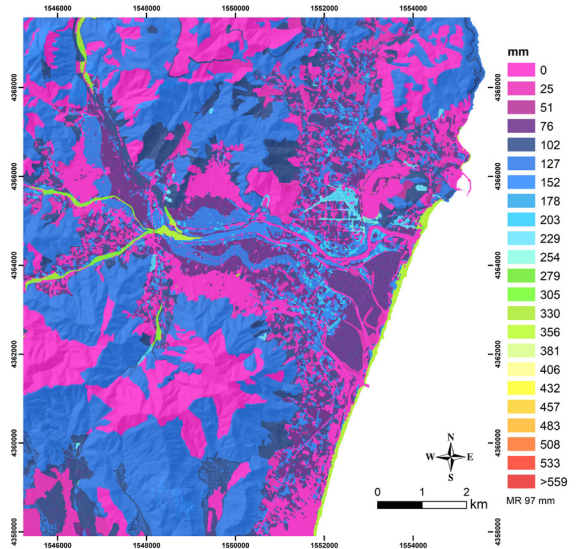

Fig. 7 -   Map of the average charge (expressed in mm per year) of the area of interest for the years 2006 to 2018 obtained by SWB. LEGEND: MR) Mean Recharge

CONCLUSIONS

The study on the soils of the Muravera area, conducted through in situ tests and laboratory analysis, has permitted to provide additional data on the hydrological characteristics of the local soils. Several parameters were determined, such as porosity and texture of soils, and the field-saturated hydraulic conductivity along the plain.

Agricultural practices, grazing and saturation grade of the soils influence the infiltration rate. Indeed, under the same texture conditions, soils in ploughed land showed a higher saturated conductivity, while soils subjected to trampling by animals showed a lower infiltration rate. It decreases as saturation grade increases.

The data obtained from in situ and laboratory tests led to the creation of the necessary inputs for the implementation of the SWB code.

The average annual recharge on a yearly base and on a longer period of 12 years was then assessed by the SWB which considered the properties of the soil and its use. This allowed to evaluate the areas of greatest infiltration and therefore to identify those in which the greatest direct recharge of the groundwater body takes place.

From the calculated hydrogeological balance, the most permeable zones are those where the Quaternary deposits crop out, where the precipitation results to have a greater infiltration rate. The grid files required allowed to know the spatialization of different data and then to increase the level of knowledge of the study area. One of the biggest advantages of SWB is its simplicity and speed of use. Although the SWB does not consider the unsaturated-zone flow, in the Muravera plain the groundwater level depth does not exceed 2-3 meters, thus one can assumes that the lag between the time when SWB generates recharge and the time when that recharge actually reaches the water

table may be not significant.

The application of SWB to the Muravera plain is an important test of the model's capability to estimate the recharge in a Mediterranean area of various land use, and in general high infiltration capacity. This method is suitable for application in similar areas and cases.

These results are very useful to better manage the water resources of the plain.

ACKNOWLEDGMENT

REFERENCES

AFRASINEI G.M., MELIS M.T., BUTTAU C., BRADD J.M., ARRAS C. & GHIGLIERI G. (2015) - *Diachronic analysis of salt-affected areas using remote sensing techniques: the case study of Biskra area, Algeria.* In: Proc. SPIE 9644, Earth Resources and Environmental Remote Sensing/GIS Applications VI, 96441D (October 20, 2015); DOI:10.1117/12.2194998.

AGRIS, LAORE, UNIVERSITÀ DEGLI STUDI DI CAGLIARI E SASSARI. (2014) - *Carta delle Unità di Terre alla scala 1:50.000-Muravera-Villaputzu-Castiadas.* http://www.sardegnaportalesuolo.it/cartografia/carte-dei-suoli/carta-delle-unita-di-terre-cut-alla-scala-150000.html.

ARDAU F. & BARBIERI G. (2000) - *Aquifer configuration and possible causes of salination in the Muravera plain (SE Sardinia, Italy).* In Proc. of 16th Salt Water Intrusion Meeting, Miedzyzdroje-Wo lin Island, Polonia (11-18).

BARLOW P.M. & REICHARD E.G. (2010) - *Saltwater intrusion in coastal regions of North America.* Hydrogeol. J., **18** (1): 247-260.

CALZOLARI C., UNGARO F. & VACCA A. (2021) - *Effectiveness of a soil mapping geomatic approach to predict the spatial distribution of soil types and their properties.* Catena **196**, 104818.

CHEMINGUI A., SULIS M. & PANICONI C. (2015) - *An assessment of recharge estimates from stream and well data and from a coupled surface-water/groundwater model for the des Anglais catchment, Quebec (Canada).* HydrogeologyJ., **23** (8): 1731-1743.

COLOMBANI N., OSTI A., VOLTA G. & MASTROCICCO M. (2016) - *Impact of climate change on salinization of coastal water resources.* Water Resour. Manag., **30** (7): 2483-2496.

CRAMER W., GUIOT J., FADER M., GARRABOU J., GATTUSO J.P., IGLESIAS A., LANGE M.A., LIONELLO P., LLASAT M.C., PAZ S., PEÑUELAS J., SNOUSSI M., TORETI A., TSIMPLIS M.N. & XOPLAKI E. (2018) - *Climate change and interconnected risks to sustainable development in the Mediterranean.* Nat. Clim. Chang., **8**: 972-980.

CRONSHEY R. (1986) - *Urban hydrology for small watersheds.* Us dept. Of agriculture, soil conservation service, engineering division.

DRIPPS W.R. (2003) - *The spatial and temporal variability of groundwater recharge within the trout lake basin of northern Wisconsin: Madison. Wis.,* University of Wisconsin.

EIJKELKAMP COMPANY (2012) - *Double ring infiltrometer operating instructions.* Giesbeek, Nederland. https://www.eijkelkamp.com/files/media/gebruiksaanwijzingen/en/m1-0904eringinfiltrometer.pdf.

IUSS WORKING GROUP WRB (2015) - *World Reference Base for Soil Resources 2014, update 2015. International soil classification system for naming soils and creating legends for soil maps.* World Soil Resources Reports No. **106**. FAO, Rome.

JIE Z., VAN HEYDEN J., BENDEL D. & BARTHEL R. (2011) - *Combination of soil-water balance models and water-table fluctuation methods for evaluation and improvement of groundwater recharge calculations.* Hydrogeology J., **19**(8): 1487-1502.

KOSTIAKOV A.N. (1932) - *On the dynamics of the coefficients of water percolation in soils and on the necessity of studying it from a dynamic point of view for purpose of amelioration.* Transactions of the 6th Communication of the Int. Society of Soil Sciences, Part A, 17–21.

MASON M. (1999) - *Le piane costiere di San Priamo e Muravera: Geologia delle coperture Quaternarie, geopedologia ed alcuni aspetti applicativi.* Tesi di laurea, Università degli Studi di Cagliari.

MATHER P. & TSO B. (2001) - *Classification Methods for Remotely Sensed Data (1st ed.).* CRC Press. https://DOI.org/10.1201/b12554.

NIGRELLI G. (2000) - *Velocità di infiltrazione dell'acqua nel terreno.* Tratto da naturaweb: Www.naturaweb.net/pdf/velinf.pdf.

NIMMO J.R., HEALY R.W. & STONESTROM D.A. (2005) - *Aquifers recharge.* In: Anderson mg, bear j (eds) encyclopedia of Hydrological Science. Wiley, Chichester, UK, 2229-2246.

RICHARDS J. (1999) - *Remote Sensing Digital Image Analysis.* Berlin: Springr-Verlag (1999), 240 p.

SCANLON B.R., HEALY R.W. & COOK P.G. (2002) - *Choosing appropriate techniques for quantifying groundwater recharge.* Hydrogeology J., **10** (1): 18-39.

Thornthwaite C.W. & Mather J.R. (1957) - *Instructions and tables for computing potential evapotranspiration and the water balance* (No. Research). Centerton.

Westenbroek S.M., Kelson V.A., Dripps W.R., Hunt R.J. & Bradbury K.R. (2010) -. *SWB a modified Thornthwaite-Mather Soil-Water-Balance Code for estimating groundwater recharge.* Reston, VA: US Department of the Interior, US Geological Survey, Ground Resources Program. 60 p.

Westenbroek S.M., Engott J.A., Kelson V.A. & Hunt R.J. (2018) - *SWB Version 2.0 A soil-water-balance code for estimating net infiltration and other water-budget components.* U.S. Geological survey techniques and methods, Book 6, Chap. **A59**, 118 p..